

Division - Soil Processes and Properties | Commission - Soil Mineralogy

Characterization and manipulation of montmorillonite properties towards technological and environmental applications

Vander Freitas Melo^{(1)*} , Regiane Salata⁽¹⁾ , Gilberto Abate⁽²⁾ , Antonio Carlos Azevedo⁽³⁾  and Larissa Kummer⁽⁴⁾ 

⁽¹⁾ Universidade Federal do Paraná, Departamento de Ciência do Solo e Engenharia Agrícola, Curitiba, Paraná, Brasil.

⁽²⁾ Universidade Federal do Paraná, Departamento de Química, Curitiba, Paraná, Brasil.

⁽³⁾ Universidade de São Paulo, Escola Superior de Agricultura Luiz Queiroz, Departamento de Ciência do Solo, Piracicaba, São Paulo, Brasil.

⁽⁴⁾ Universidade Federal Tecnológica do Paraná, Departamento de Química e Biologia, Curitiba, Paraná, Brasil.

ABSTRACT: The combination of pillarization and charge neutralization with Li⁺ can make montmorillonite an important support material for industry and decontamination of pollutants in soil and water. Montmorillonite characterization techniques were described in detail, and pillarization procedures were used, after Li⁺ saturation, to modify and manipulate the chemical and mineralogical surface properties of this montmorillonite. Eight samples were produced: 1) natural montmorillonite (Chisholm Mine - MMT); 2) Li⁺ saturated montmorillonite (MMTLi); 3) polyethylene glycol (PEG) Al-pillared montmorillonite (AIPEG); 4) PEG Al-pillared montmorillonite saturated with Li (AIPEGLi); 5) Al-pillared montmorillonite with 14 h contact time (Al14h); 6) Al-pillared montmorillonite Al14h saturated with Li (Al14hLi); 7) Al-pillared montmorillonite with 0 h contact time (Al0h); and 8) Al-pillared montmorillonite Al0h saturated with Li (Al0hLi). The natural sample was identified as interlayered montmorillonite composed of chlorite layers or with a high degree of Al-hydroxy filling. Concerning the total permanent charges, 70 % occurred by isomorphic substitution of Al³⁺ by Mg²⁺ in octahedral layer and 30 % of Si⁴⁺ by Al³⁺ in tetrahedral layer. The pillarization method using the PEG produced a small number of stable pillars. The new milder pillarization method (Al0h) did not cause damage in the formation of Al-hydroxy. In this method, the resulting pillars were more homogeneous in size. Thereby, the Al0h Li method has been shown to produce a supporting material with a constant interlayer spacing, increased of the specific surface area (SSA), and drastic reduction of the cation exchange capacity (CEC) as compared to MMT. This modified mineral can be used in, for example, decontamination of polluted water with nonionic organic pollutants.

Keywords: pillarization, Al-hydroxy interlayer, Al-pillared montmorillonite, specific surface area, cation exchange capacity.

*** Corresponding author:**

E-mail: melovander@yahoo.com.br

Received: September 20, 2020

Approved: March 12, 2021

How to cite: Melo VF, Salata R, Abate G, Azevedo AC, Kummer L. Characterization and manipulation of montmorillonite properties towards technological and environmental applications. Rev Bras Cienc Solo. 2021;45:e0200149. <https://doi.org/10.36783/18069657rbcs20200149>

Editors: José Miguel Reichert , Leônidas Azevedo Carrijo Melo  and Laurent Caner .

Copyright: This is an open-access article distributed under the terms of the Creative Commons Attribution License, which permits unrestricted use, distribution, and reproduction in any medium, provided that the original author and source are credited.



INTRODUCTION

Montmorillonite has a high specific surface area (SSA), high cation exchange capacity (CEC), and is the most common 2:1 phyllosilicate in temperate soils (Borchardt, 1989). Even in a small amount, it interferes expressively in the chemical and physical soil properties. Therefore, the proper identification of the smectite is fundamental.

Montmorillonite belongs to the smectite group, which can be divided into dioctahedral (montmorillonite, beidellite, and nontronite) and trioctahedral (hectorite, saponite, and sauconite) sub-groups (Barnhisel and Bertsch, 1989). Within both the di- and trioctahedral subgroups, the structural charge is originated from heterovalent isomorphic substitution in the tetrahedral and/or the octahedral sheets (Bujdák, 2006). The isomorphic substitution of Al^{3+} per Mg^{2+} into the dioctahedral sheet of montmorillonite (Czímerová et al., 2006; Kaufhold, 2006; Sun et al., 2016) produces a negative charge excess of $-1/6$ in each of the six oxygens coordinated with Mg, which results in the formation of -1.0 negative charge in each substituted octahedra ($6 \times -1/6 = -1.0$). The charges created by isomorphic substitution are called permanent charges, in opposition to the variable charges at the particle edges, created by the dissociation of OH groups (Sposito, 1989).

This excess of negative charge propagates to the four apical oxygens, which are shared between the substituted octahedra and the Si tetrahedra of adjacent tetrahedral sheets (two in the upper and two in the lower sheet) (Johnston and Tombácz, 2002). Since the origin of the permanent charge is far inside the mineral, the electric field reaching the external surfaces is wider and weaker than the field originated from isomorphic substitution in tetrahedral sheets (Moore and Reynolds Jr, 1997).

The presence of an electric field into the montmorillonite interlayers makes it a thermodynamically unfavorable environment for uncharged, hydrophobic molecules to escape from aqueous solutions (Johnston and Tombácz, 2002). However, due to the dioctahedral nature of montmorillonite, it is possible to neutralize the permanent negative charges caused by the octahedral isomorphic substitution by inserting a Li^+ ion into the empty octahedra (Greene-Kelly, 1953; Lim and Jackson, 1986). As a consequence, the dioctahedral sheet would have two Al^{3+} and one Li^+ for every three octahedral positions (Volzone, 1991), turning it into a non-expansive, near-zero structural charge mineral (Greene-Kelly, 1953).

Another way to manipulate the characteristics of montmorillonite is by controlling the basal spacing of the mineral via pillarization. The pillarization consists of precipitating Al-hydroxy polymers into the montmorillonite interlayers (Bertsch, 1987; Sartor et al., 2015; Liu et al., 2018; Wen et al., 2019). The Al-hydroxy compromise the expansivity and reduce the CEC of smectites (Barnhisel and Bertsch, 1989; Mnasri-Ghnimi and Frini-Srasra, 2019). The formation of 2:1 minerals with Al-hydroxy makes these minerals more resistant to weathering (Karathanasis and Hajek, 1984).

Although the natural occurrence of Al polymers in the interlayers of 2:1 phyllosilicates is of great pedological interest, it was in the controlled synthesis of polymers and their insertion in the interlayers that the greatest advances have occurred in the last decades (Moma et al., 2018). These advances are justified, in general terms, by the resulting surprising great catalytic properties that emerge from this manipulation, which are very interesting in the petrochemical cracking process (Tomlinson, 1998), for example. In a parallel approach, the handling of charges and basal spacing (or porosity) of 2:1 phyllosilicates has various environmental applications such as the retrieval of potentially toxic element and undesirable, apolar organic molecules (Tomlinson, 1998; Sartor and Azevedo, 2014; Sartor et al., 2015; Liu et al., 2018; Mnasri-Ghnimi and Frini-Srasra, 2019; Chauhan et al., 2020).

The hydroxy-Al species structure is thought to be of two types: 1) gibbsite-like sheets, or 2) polyoxometalates ions, particularly the Keggin ion (Wen et al., 2019). The literature reports that, in pedogenic hydroxy interlayered smectites (HIS), the interlayer spacing tends to be fixed at approximately 1.4 nm. Variability in this spacing depends on the degree of Al occupation, commonly resulting in changes in symmetry/asymmetry of the 1.4 nm peak than in the actual peak position (Meunier, 2007).

On the other hand, montmorillonites synthetically pillarized have been reported to have 1.8 nm spacing (Liu et al., 2018; Wen et al., 2019). One of the main pillarization agents is the polycation $[Al_{13}O_4(OH)_{24}(H_2O)_{12}]^{7+}$ (Sartor et al., 2015). This is also named Al_{13} or Keggin ion and consists of 12 octahedrally and one tetrahedrally coordinated aluminum ions, usually obtained by hydrolysis of an aluminum chloride solution (Lahav et al., 1978; Selvaraj et al., 1996). Due to its high charge (7+), the Al_{13} easily replaces other interlamellar cations in the interlayer positions (Vaughan, 1988). Keggin- Al_{30} also has been used to produce pillared montmorillonite (Wen et al., 2019). The Al-pillared montmorillonite not only has unique microporous structural characteristics, excellent thermal stability, and a large specific surface area, but it also catalyzes reactions of different organic and inorganic compounds (Gao et al., 2014; Georgescu et al., 2018).

We hypothesized that, despite the Al pillars structure, the combination of pillarization and charge neutralization with Li^+ has great potential to make montmorillonite an important support material to be used in environmental decontamination of nonionic organic pollutants. To check this hypothesis, a montmorillonite sample was fully characterized, and different pillarization procedures were used, followed by Li^+ saturation, in order to modify the chemical and mineralogical characteristics of the mineral towards this end.

MATERIALS AND METHODS

The study was carried out using a commercial sample of bentonite (montmorillonite-rich sedimentary rock), from Chisholm Mine, Polkville, Mississippi, USA. Except for particle size analysis, the samples used were all dried in an oven at 40 °C and grounded using a pestle and mortar to pass through a 0.20 mm sieve.

Characterization techniques of montmorillonite

The particle size analysis was done using the pipette method (Gee and Bauder, 1986). Approximately 4 g of the sample was dispersed by shaking it for two hours into 40 mL of a combined solution of 0.6 mol L⁻¹ sodium hexametaphosphate and sodium carbonate 0.07 mol L⁻¹. The sand fraction was retained in a 0.053 mm sieve, and the silt and clay fractions were separated based on sedimentation rates, according to the Stokes's law (Gee and Bauder, 1986).

To confirm the smectitic nature of the sample, it was saturated with Mg^{2+} , Mg^{2+} + ethylene glycol, K^+ , and K^+ + heating at 550 °C (Witthig and Allardice, 1986). The change in the interlayer spacing after these treatments was measured in X-ray diffractograms. The sample was also treated with boiling NaOH 0.5 mol L⁻¹ to identify possible interstratification with chlorite layers or with layers with a high degree of filling with Al-hydroxy (Lim and Jackson, 1986). This alkaline extraction removes aluminosilicates of low crystallinity and dissolves the Al-hydroxy in the interlayers of 2:1 minerals (Melo et al., 2002). The NaOH-treated sample was then saturated with K^+ and heated to 500 °C.

After identifying the smectite, the Greene-Kelly test (Greene-Kelly, 1953; Lim and Jackson, 1986) was used to identify the nature of mineral within the smectite group: dioctahedral (montmorillonite) or trioctahedral. All X-ray diffractograms were recorded using a Panalytical X'Pert3 Powder equipped with a vertical goniometer (40 kV, 40 mA CuK α radiation at 0.15418 nm) in the range 3 to 30 °2 θ , with an angular speed of 0.4 °2 θ s⁻¹.

The diffractometer was equipped with Xcelerator Scientific detector and a Ni filter. Samples were irradiated as oriented mounts.

Manipulation of the basal distance of montmorillonite (Al-pillarization)

Two intercalation procedures were employed (Figure 1). The first one used polyethylene glycol 400 (PEG) as the expanding agent of the mineral sheets (Gao et al., 2014). In the second one, an intercalating solution containing exchangeable ions Al_{13} (Keggin ion; Figure 2) was used, in the absence of PEG (Romero-Pérez et al., 2012), and varying the aluminum concentration and contact time. The standard method proposed by Romero-Pérez et al. (2012) uses an intercalating solution of $AlCl_3$ 0.2 mol L^{-1} and $NaOH$ 0.5 mol L^{-1} , one-hour agitation, and contact time of 14 h (Al14h). To reduce the preparation time, in the present study, a milder intercalation method was tested: $AlCl_3$

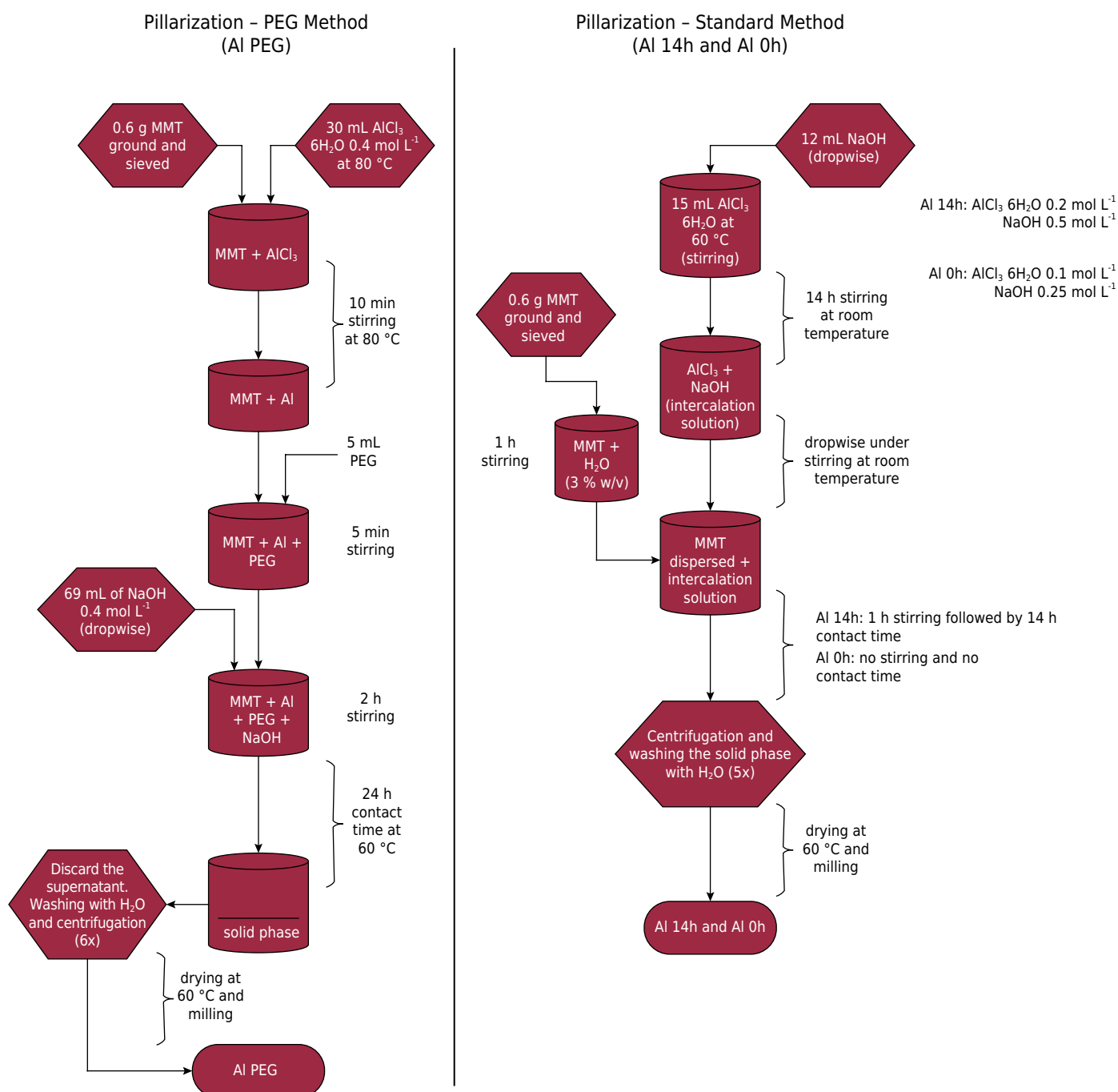


Figure 1. Pillarization processes with and without polyethylene glycol (PEG).

0.1 mol L⁻¹ and NaOH 0.25 mol L⁻¹, without shaking and without contact time at the end of the process (Al0h).

To test the stability of the Al-hydroxy produced by the three treatments (PEG, Al14h, and Al0h), the pillared samples were oriented onto slides, heated to 60, 350, and 550 °C, and studied by XRD. The crystallite sizes of natural montmorillonite (K⁺ + 550 °C) and pillared montmorillonite (60 and 550 °C) were calculated from the width at half-height of the reflection (001) (Klug and Alexander, 1954; Melo et al., 2002).

Manipulation of the permanent montmorillonite charge

Aliquots of the natural montmorillonite and Al-pillared montmorillonite by the three treatments were saturated with Li⁺ (Greene-Kelly, 1953; Lim and Jackson, 1986) to neutralize the permanent octahedral charges (Figure 2).

After pillarization and saturation with Li, removing salts excess and Al compounds was ensured by suspending the samples in deionized water and transferring them into a dialysis membrane (Sigma-Aldrich, reference number D9527), which were soaked in deionized water for three weeks, with daily water renew.

At the end of these procedures, eight samples were produced: 1) natural montmorillonite extracted from Chisholm Mine, Polkville, Mississippi (MMT); 2) Li saturated montmorillonite (MMLi); 3) polyethylene glycol (PEG) Al-pillared montmorillonite (AIPEG); 4) PEG Al-pillared montmorillonite saturated with Li (AIPEGLi); 5) Al-pillared montmorillonite with 14h contact time (Al14h); 6) Al-pillared montmorillonite Al14h saturated with Li (Al14hLi); 7) Al-pillared montmorillonite with 0h contact time (Al0h); and 8) Al-pillared montmorillonite Al0h saturated with Li (Al0hLi).

Evaluations of treated samples

Cation exchange capacity (CEC)

The eight samples were previously adjusted to pH 6.0 by adding solutions of HCl 0.5 mol L⁻¹ or NaOH 0.2 mol L⁻¹. Approximately 0.3 g of sample was oven-dried (40 °C

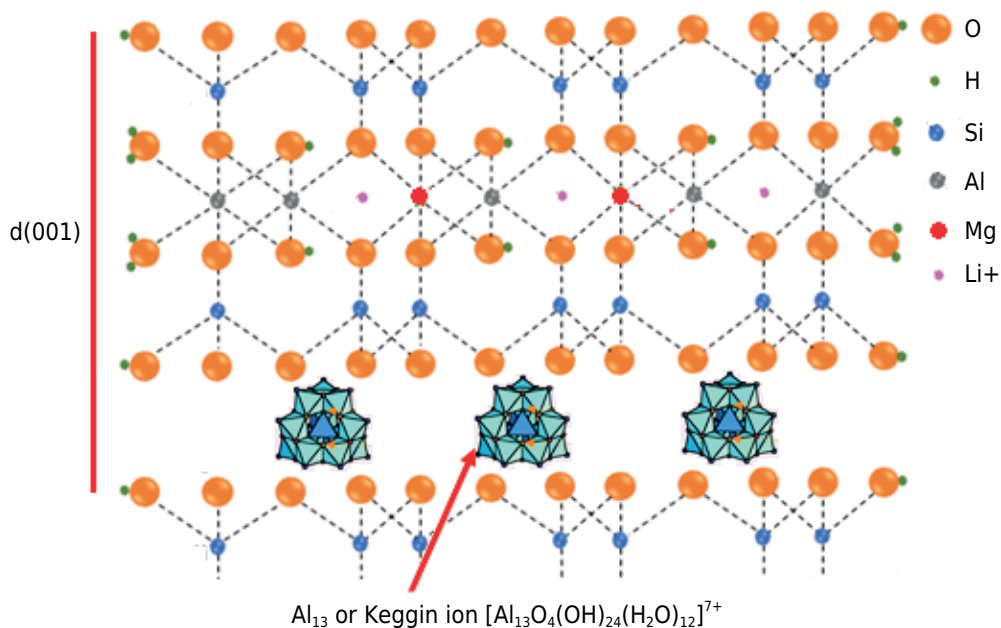


Figure 2. Schematic representation of basic 2:1 layer of montmorillonite (Mt) (isomorphic substitution of Al³⁺ for Mg²⁺ in the octahedral sheet), Al-pillarized (AIPEG, Al14h, and Al0h) and saturated with Li⁺ (AIPEGLi, Al14hLi, and Al0hLi).

for 24 h), in triplicate, held in contact for 10 min with 3 mL of MgCl_2 0.2 mol L^{-1} solution and then centrifuged at 3000 rpm. This procedure was repeated three times in total. The solid fraction was then washed eight times with deionized water until the AgNO_3 test (1.0 mol L^{-1}) resulted negative for AgCl precipitation (absence of soluble Cl^-).

Then, 3 mL of BaCl_2 0.2 mol L^{-1} were added, and the mixture was stirred for 20 min and centrifuged at 3000 rpm for 15 min. The concentration of Mg in the extract was determined using a Varian AA240FS atomic absorption spectrophotometer, in a current of 10 mA and acetylene gas. The CEC was determined by the concentration of Mg^{2+} desorbed from samples by Ba^{2+} .

Specific surface area

The specific surface area (SSA) was determined by the BET method (Brunauer - Emmett - Teller) - N_2 in Quantachrome NOVA 4000e equipment.

Scanning electron microscopy (SEM) and energy dispersive spectrometer (EDS)

Non-polished samples were analyzed with a Tescam VEGA 3 LMU and EDS-SEM Oxford X-Max, with a detector 80 mm^2 - Silicon, drift detector. Analytical conditions were 15 kV and 15 mm working distance. Count rates were adjusted to give >15 - 20 kcps and beam intensity calibrated on a pure Cu standard. Images obtained in backscatter electron mode allowed the identification of areas with different atomic numbers. The average detection limit (light and heavy elements) of EDS was 0.5 % (w/w).

The chemical formulas of natural MMT were calculated from individual crystals (EDS) and considering the theoretical montmorillonite formula ($\text{R}_{0.33}^+(\text{Al}_{1.67}\text{Mg}_{0.33})\text{Si}_4\text{O}_{10}(\text{OH})_2$) (Hetzel and Doner, 1993). It was used the average chemical composition of 15 montmorillonite particles. The calculation was based on the charge balance of structural charges (number of negative charges of the ideal formula was $10 (\text{O}^{2-}) + 2 (\text{OH}^-) = 22^-$), and the predicted coordination of cations in the structure (by the ratio of radii between cations and oxygen, considering the following structural element loci: Si^{4+} - tetrahedral; Al^{3+} - tetrahedral and octahedral; Mg^{2+} - octahedral; Fe^{3+} - octahedral). The Ca^{2+} cation was not considered in the layers structure because it stabilizes the cubic coordination (Hetzel and Doner, 1993).

To convert the negative charge resulting from isomorphic substitutions per unit of formula (charge equivalent (-) per unit of formula) to CEC ($\text{cmol}_c \text{kg}^{-1}$), the procedures described in Kaufhold (2006), Hetzel and Doner (1993), and Batista et al. (2017) were followed.

RESULTS

Characterization of montmorillonite

The starting sample was composed mainly of particles in the silt (68 %), followed by the clay (31 %), and sand (1 %) fractions. A peak at 1.56 nm, typical of 2:1 phyllosilicates, was observed in all fractions (Figure 3). In the sand fraction, the 1.56 nm peak was less intense due to the great amount of and high crystallinity of quartz.

According to the treatments (Mg^{2+} , Mg^{2+} + ethylene glycol, K^+ , and K^+ + heating at 550 °C), the change in basal distance of the MMT samples is shown in figure 4. The highest intensity peak corresponds to the MMT (untreated sample). When saturated with Mg^{2+} , the MMT presented basal spacing of 1.55 nm, close to the natural sample spacing. After saturation with ethylene glycol, the d(001) peak increased to 1.79 nm, confirming it was a highly expandable 2:1 mineral of the smectite group (Witthig and Allardice, 1986). This result also rejected the occurrence of hydroxy interlayer smectite (HIS) or chlorite in separate phases, in which case there would be two isolated peaks at 1.51 and 1.79 nm.

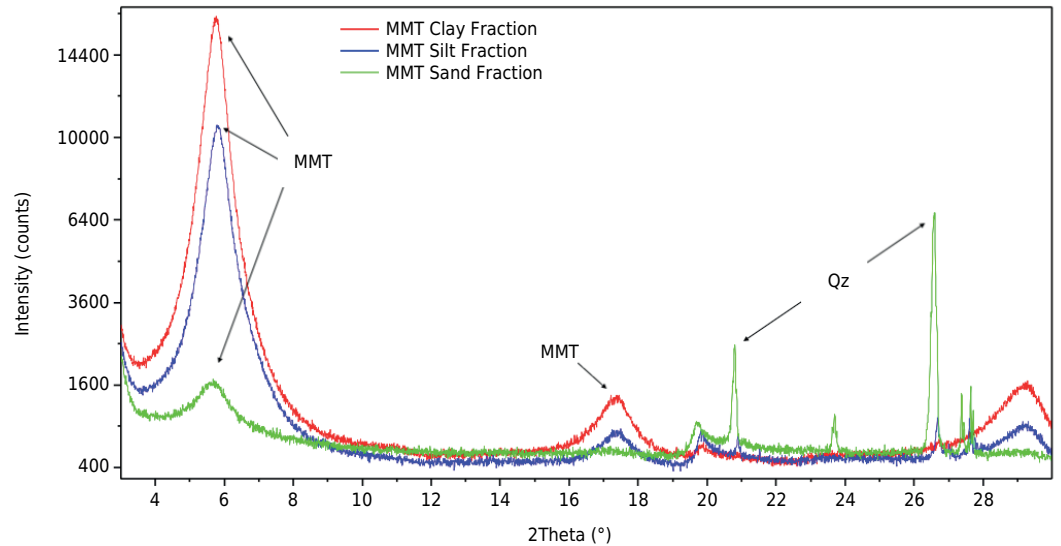


Figure 3. XRD of sand, silt, and clay fractions of the montmorillonite sample.

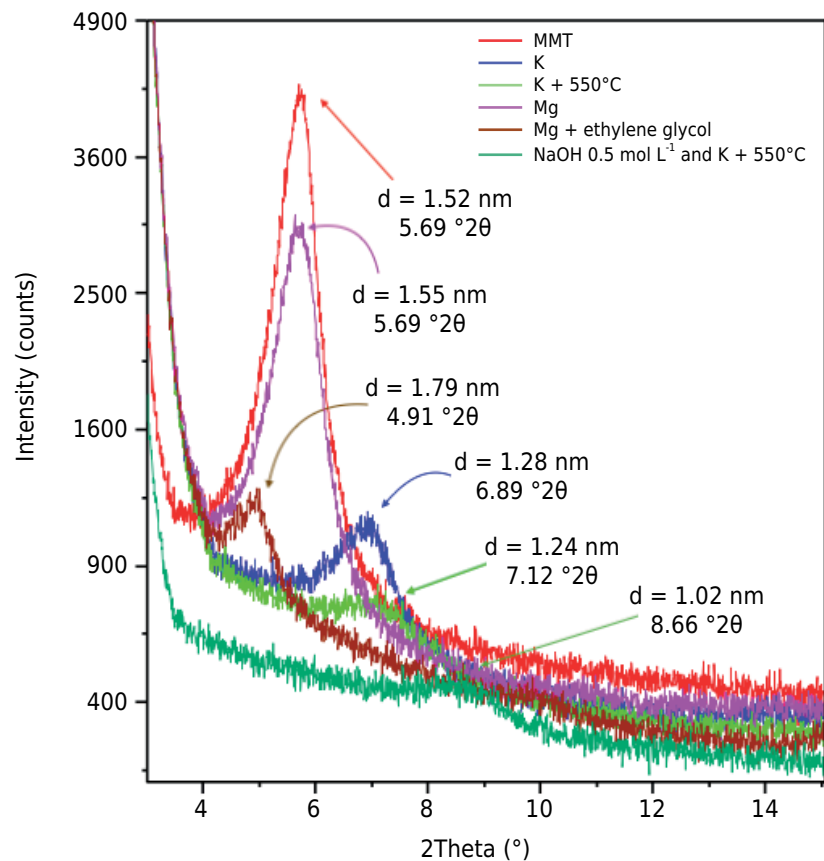


Figure 4. XRD of the sample submitted to the treatments with Mg^{2+} , Mg^{2+} ethylene glycol, K^+ , and K^+ + 550 °C and extraction with NaOH followed by saturation K^+ + heating at 550 °C.

After saturation with K^+ , the basal spacing was reduced to 1.28 nm, also rejecting the presence of vermiculite, which would have the $d(001)$ peak reduced to near 1.0 nm (Witthig and Allardice, 1986). Heating of the K^+ sample at 550 °C resulted in a partial collapse of the mineral to 1.24 nm (Figure 4). Because the collapse was not complete to 1.0 nm, regular interstratifications of the smectite with chlorite layers or with Al-hydroxy filling should occur. This interstratification was confirmed because the treatment with NaOH 0.5 mol L⁻¹ for removal of the interlayered Al-hydroxy (Melo et al., 2002) followed by K^+

+ 550 °C, caused the layers to collapse to 1.0 nm (Figure 4). Thus, these treatments outcome confirmed the MMT sample was a smectite interstratified with layers of chlorite or layers with a high degree of Al-hydroxy filling.

The MMT d(001) spacing decreased from 1.52 nm to 0.95 nm (Figure 5) when saturated with Li⁺ (Greene-Kelly, 1953), which remained unchanged after solvation with ethylene glycol, i.e., the mineral lost its expansion capacity, which is typical of no- or low-charged dioctahedral phyllosilicates (montmorillonite). The mean crystal diameter (MCD) of MMT treated with K⁺ + 550 °C was 6.17 nm (Table 1). Considering the d(001) of this treatment was 1.24 nm, because the collapsed layers were only propped by the layers of chlorite or interstratified Al-hydroxy, the MMT particles had five 2:1 layers (6.17 / 1.24 = 5).

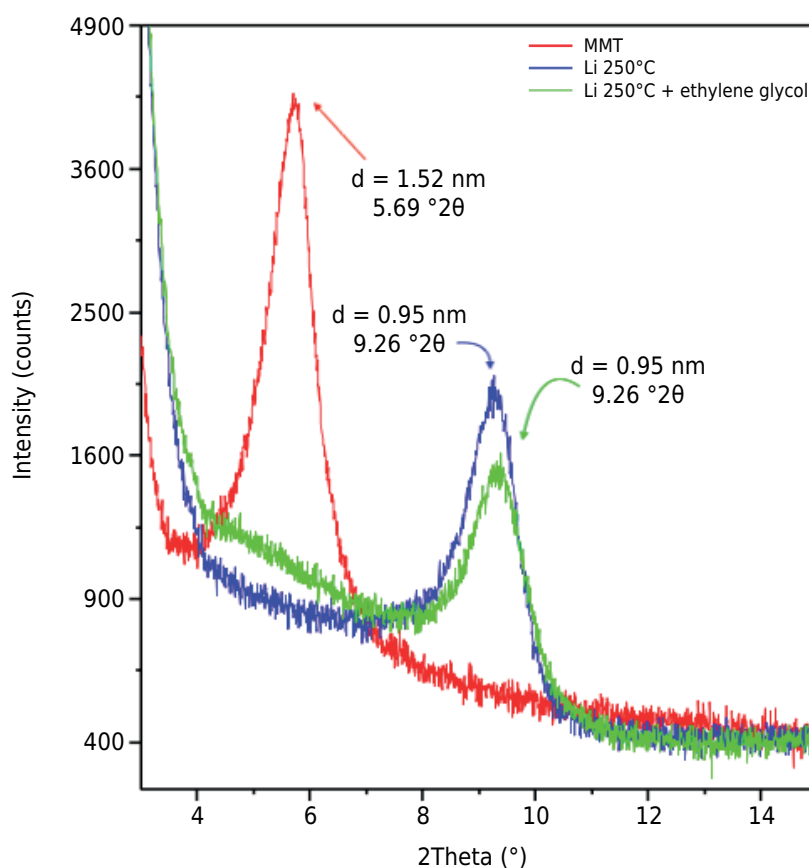


Figure 5. XRD of the natural montmorillonite sample submitted to the Greene Kelly test.

Table 1. Crystallographic data of the samples

Sample	A		B		C=A-B ⁽¹⁾	D ⁽²⁾		E=A-D ⁽³⁾	F=(C/D) × 100	G=100-F ⁽⁴⁾	FWHM ⁽⁵⁾	MCD ⁽⁶⁾
	d(001) 60 °C	d(001) 550 °C	d(001) 550 °C	d(001) 550 °C		nm	nm					
MMT				1.240							1.31	6.17
Al PEG	1.794	1.596	0.198			0.554	36	64	1.09	7.48		
Al 14h	1.918	1.822	0.096			0.678	14	86	0.80	10.47		
Al 0h	1.875	1.810	0.065			0.635	10	90	0.93	8.87		

⁽¹⁾ C: reduction of the basal distance of the pillared minerals between the heating at 60 and 550 °C. ⁽²⁾ D: basal distance of MMT K⁺ + 550 °C.

⁽³⁾ E: reduction of the basal distance of pillared minerals in relation to MMT K⁺ + 550 °C. ⁽⁴⁾ G: the degree of occupation of the Al-hydroxy.

⁽⁵⁾ FWHM: full width at half maximum reflection (001). ⁽⁶⁾ MCD: mean crystal diameter in the (001) plan.

Manipulation of the montmorillonite basal distance (Al-pillarization)

The values of $d(001)$ ranged from 1.80 to 1.90 nm (Table 1 and Figure 6). There was no peak at 0.484 nm, which indicates no formation of gibbsite in the pillared samples. The contact time of 14 h as compared to 0 h caused an increase in basal spacing [$d(001)$ (60 °C) (Table 1)]. The untreated MMT saturated with Li^+ and heated at 250 °C (Greene-Kelly, 1953) shifted the peak to 0.97 nm (Figure 7). This collapse of the layers was due to the neutralization of the negative charges by Li^+ in the octahedral sheet. The pillarization

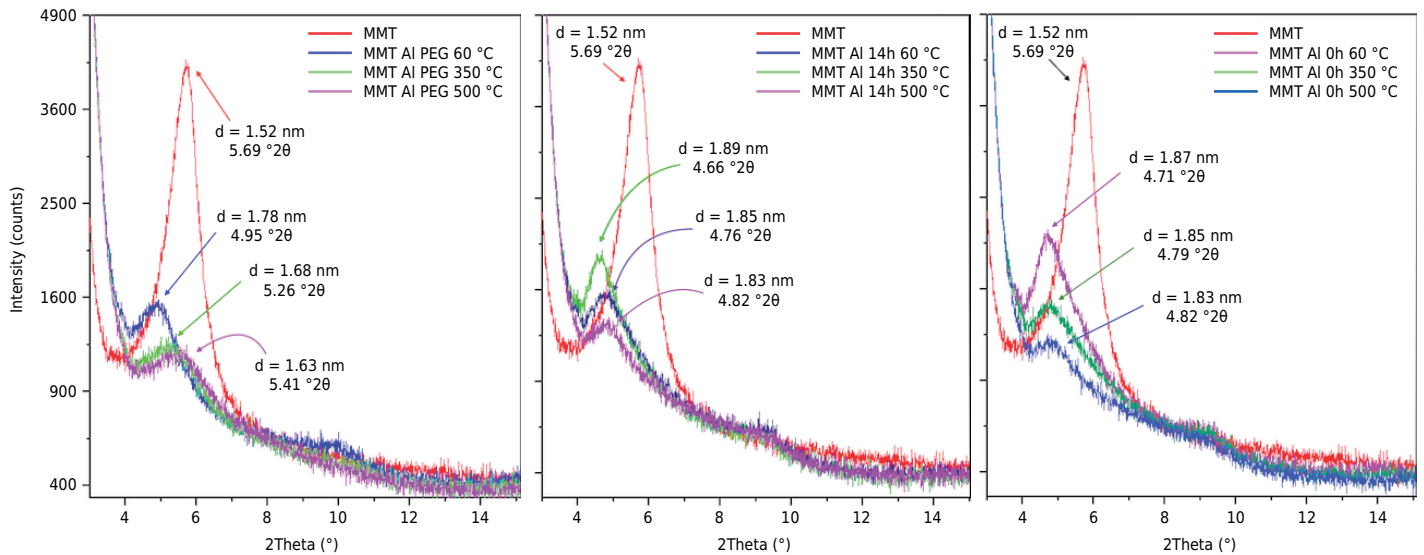


Figure 6. XRD samples of AlPEG (a), Al14h (b), and Al0h (c) heated to 60, 350, and 500 °C compared to natural MMT.

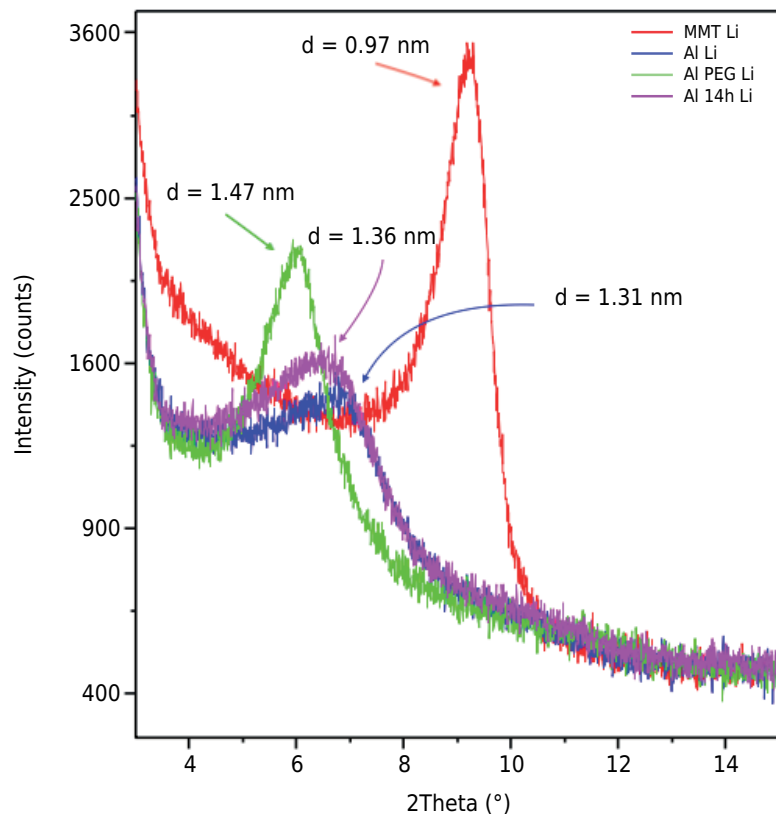


Figure 7. Comparative XRD between MMT and pillar samples, all saturated with Li^+ and heating at 250 °C.

in the Al PEG, Al 14h, and Al 0h samples prevented the collapse of the structures, even after heating at 250 °C (Al0h - 1.31 nm; Al 14 h - 1.36 nm; AlPEG - 1.47 nm).

Evaluation of manipulating montmorillonite properties

Scanning electron microscopy

As an example of crystal morphology, micrographs of MMT samples (Figure 8a) and Al0hLi (Figure 8b) are presented. Many particles with a size close to 5 µm could be identified, which was compatible with the predominance of the silt fraction in the particle size analysis. The EDS analysis showed an increase of Al content in the pillared samples (Table 2). The Li (Z = 3) cannot be detected in the saturated samples because the EDS sensor only detects elements with atomic number higher than carbon (Z = 6).

The MMT formula, based on the microchemical EDS analysis (Table 2 - mean values of 15 particles) and other premises described by Hetzel and Doner (1993), was $\text{Ca}_{0.3}(\text{Al}_{1.19}\text{Fe}_{0.40}\text{Mg}_{0.4})\text{Si}_{3.82}\text{Al}_{0.18}\text{O}_{10}(\text{OH})_2$. The sum of negative charges due to isomorphic substitutions in the tetrahedral and octahedral sheets was 0.6 mol or CEC per unit of formula ($0.18^- + 0.41^- \sim 0.6^-$), neutralized by 0.3 mol of Ca^{2+} ($0.3 \times 2^+ = 0.6^+$). The

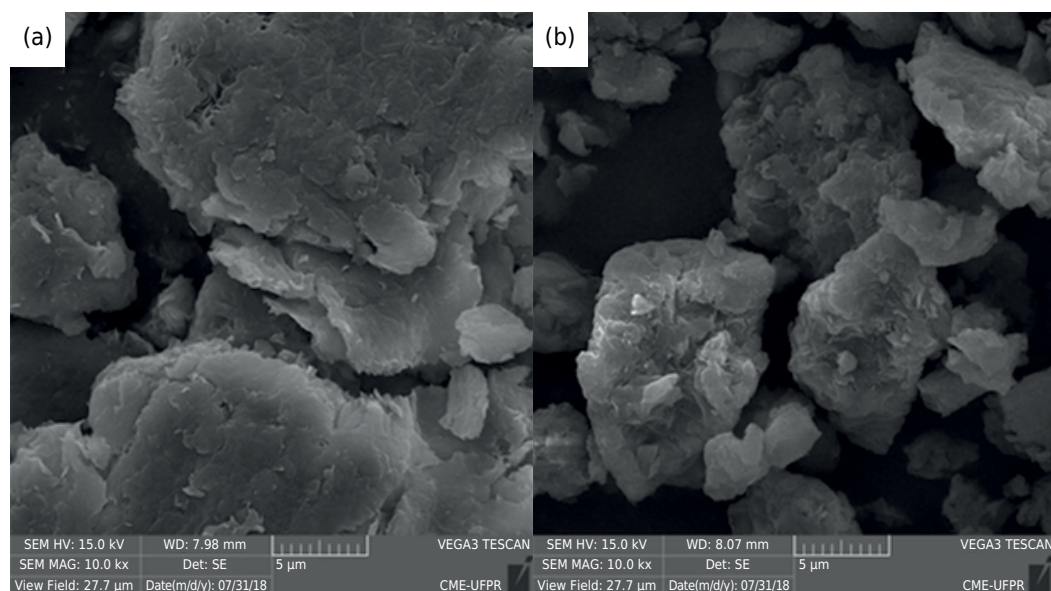


Figure 8. Sample scanning electron microscope (SEM) micrographs of natural MMT (a) and Al0h Li (b).

Table 2. Results of chemical composition (EDS) of the samples (mean values of analysis of 15 particles)

Sample	O	Si	Al	Fe	Mg	Ca
	%(¹)					
MMT	53.9	27.9	10.0	2.9	3.0	1.9
MMT Li	51.7	30.6	10.7	3.9	2.9	nd ⁽²⁾
AlPEG	54.5	24.6	15.9	2.7	2.3	nd
AlPEG Li	53.9	25.7	14.9	3.1	2.4	nd
Al14h	54.3	25.8	14.3	3.4	2.4	nd
Al14h Li	54.4	26.9	12.9	3.1	2.6	nd
Al0h	55.1	25.1	13.9	3.2	2.5	nd
Al0h Li	53.3	27.8	13.0	3.3	2.6	nd

⁽¹⁾ w/w. ⁽²⁾ nd: below detection limit (0.5 %).

contribution of the isomorphous substitution in the octahedral and tetrahedral sheets was 70 % $[(0.41 / 0.6) \times 100]$ and 30 % $[(0.18 / 0.6) \times 100]$, respectively. Following the procedures of Hetzel and Doner (1993) and Kaufhold (2006) to convert the structural CEC per unit of formula (0.6) to CEC per kg of the mineral resulted in 0.1063 equivalent (eq) of (-) 100 g^{-1} or $106 \text{ meq } 100 \text{ g}^{-1}$ or $106 \text{ cmol}_c \text{ kg}^{-1}$.

Specific Surface Area

The untreated MMT SSA was $69 \text{ m}^2 \text{ g}^{-1}$ (Figure 9). The Al-hydroxy pillarization caused a significant increase in SSA regardless of the method used. The SSA was greater in Al14h ($165 \text{ m}^2 \text{ g}^{-1}$) and Al0h ($152 \text{ m}^2 \text{ g}^{-1}$) than the AlPEG ($134 \text{ m}^2 \text{ g}^{-1}$) sample. There was no significant difference in SSA between samples produced by the Al14h and the Al0h treatments. The saturation with Li in samples Al14h and Al0h reduced the SSA as compared to their non-Li equivalents (Figure 9).

Cation Exchange Capacity

The untreated MMT CEC was $85 \text{ cmol}_c \text{ kg}^{-1}$ (Figure 10). The pillarization with Al-hydroxy neutralized about $21 \text{ cmol}_c \text{ kg}^{-1}$, i.e., 20 % of the original theoretical CEC of the mineral. Using the EDS data (Table 2), it was found that the untreated MMT CEC should be $106 \text{ cmol}_c \text{ kg}^{-1}$. Assuming the main pillarization agent was the polycation $[\text{Al}_{13}\text{O}_4(\text{OH})_{24}(\text{H}_2\text{O})_{12}]^{7+}$ (Selvaraj et al., 1996), each pillar would block seven negative permanent charges.

The Li saturation did not neutralize all negative charges resulted from isomorphous substitution (Figure 10). If so, the MMT Li sample should only had a CEC of approximate $5 \text{ cmol}_c \text{ kg}^{-1}$ (5 % of total CEC - $106 \text{ cmol}_c \text{ kg}^{-1}$), which is the variable charge due to OH dissociation at the particle's edges (Azevedo and Vidal-Torrado, 2009); instead, it had $15 \text{ cmol}_c \text{ kg}^{-1}$. However, the estimate of the variable CEC as about $5 \text{ cmol}_c \text{ kg}^{-1}$ considers the total deprotonation of the silanol (-SiOH) and a small fraction of the aluminol groups (-AlOH) at the particle edges (Azevedo and Vidal-Torrado, 2009). Instead, the pH of all the samples was corrected to 6.0; therefore, this excess of CEC in the MMT Li sample ($10 \text{ cmol}_c \text{ kg}^{-1}$) was a consequence of the isomorphous substitution occurring in the tetrahedral sheet, which is not neutralized by the Li saturation (Jaynes and Bigham, 1987).

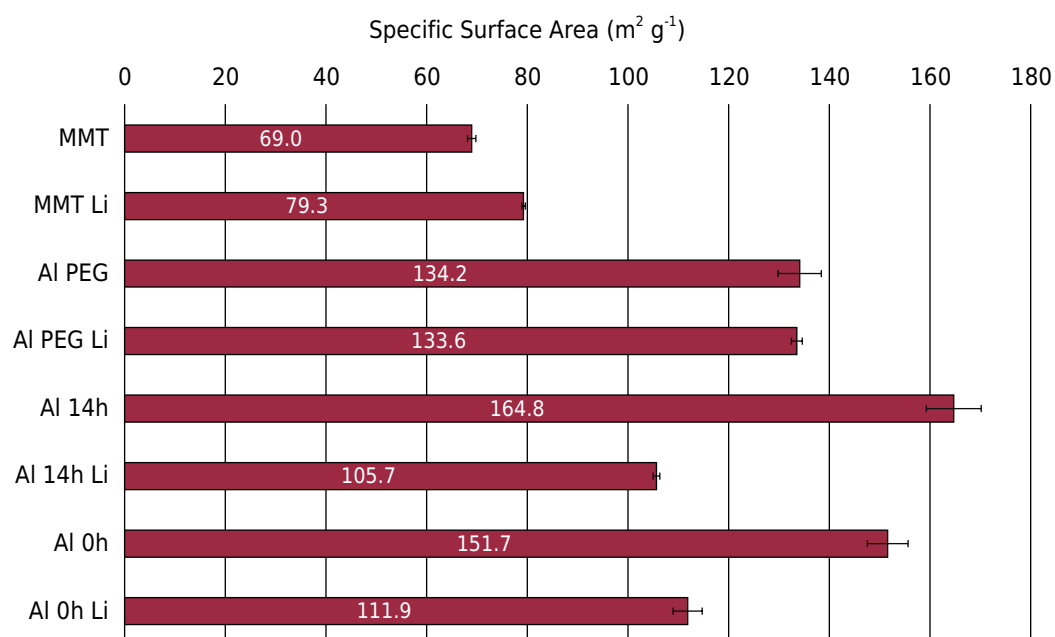


Figure 9. Specific surface area of natural MMT, Al-pillared, and saturated with Li samples. The dashes in the bars mean the standard deviation of the data.

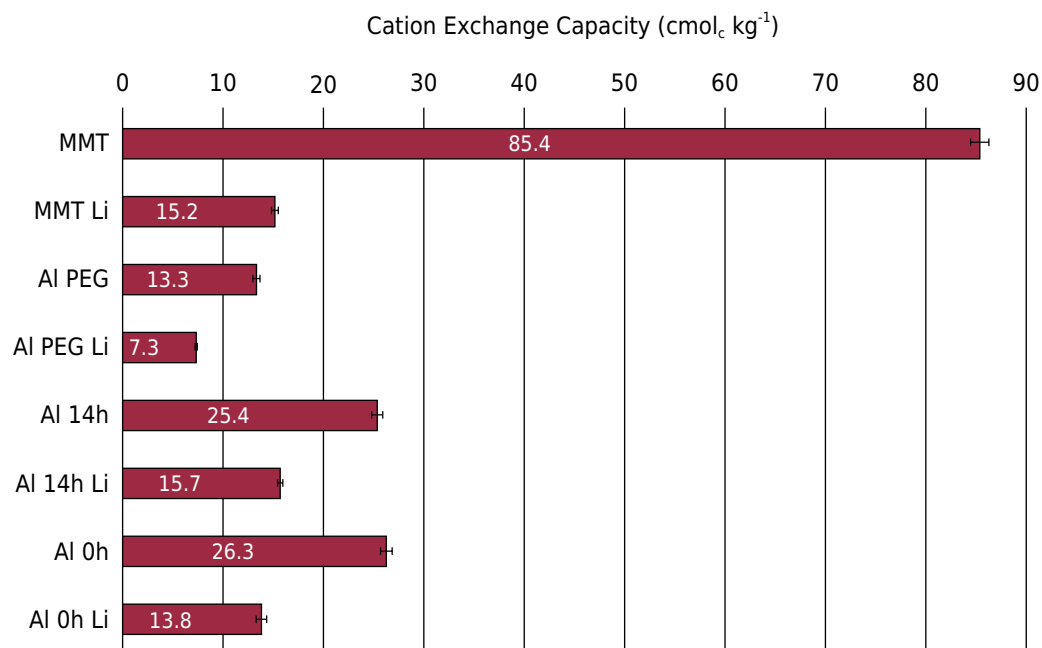


Figure 10. Cation Exchange Capacity of the samples. The dashes in the bars mean the standard deviation of the data.

The estimate based on the allocation of the element content (EDS results; Table 2) into the formula of natural MMT resulted that 30 % of its CEC was derived from isomorphous substitution in the tetrahedral sheet.

DISCUSSION

The results confirmed that the sample was a montmorillonite interstratified with layers of chlorite or layers with a high degree of filling with Al-hydroxy (MMT) (Figures 3 and 4). The Greene-Kelly test (Greene-Kelly, 1953) corroborated the sample as a montmorillonite instead of another dioctahedral smectite (beidellite, nontronite) or a trioctahedral one (saponite, hectorite, and sauconite). When the isomorphous substitution occurs in the dioctahedral sheet (Al^{3+} per Mg^{2+}), Li^+ saturation used in the Greene-Kelly test enters the vacant octahedra and neutralizes the excess of negative charge, making the mineral no longer expandable even with saturation with ethylene glycol (Jaynes and Bigham, 1987).

The values of $d(001)$ (1.80 and 1.90 nm) in the pillarized samples (Figure 5) were compatible with the formation of Keggin ions in the interlayers (Meunier, 2007; Sartor et al., 2015; Wen et al., 2019). If there are gibbsite-like layers formed, the basal spacings should be similar to that in chlorite (around 1.40 nm) (Meunier, 2007). The variations in $d(001)$ as a function of the pillarization treatments Al14h and Al0h may be related to the position of Al_{13} (Keggin ion; Figure 2) in the interlayer (Figure 5 and Table 1), since the polymer is not perfectly symmetrical (Čapková et al., 1998; Wen et al., 2019). Another possibility is that the long contact time of 14 h (aging) treatment favored the hydrolysis of Al of the Keggin ion $[\text{Al}_{13}\text{O}_4(\text{OH})_{24}(\text{H}_2\text{O})_{12}]^{7+}$, forming the Al_{13}^{5+} and Al_{13}^{3+} compounds (Bottero et al., 1982). These compounds neutralize a smaller number of permanent charges in the interlayers than the ideal Keggin. The Al_{13}^{7+} occupies eight units cells' space, neutralizing seven negative charges (Čapková et al., 1998). Instead, the hydrolyzed species (Al_{13}^{5+} and Al_{13}^{3+}) have to be in greater amount and closer to each other to neutralize the same number of charges. The closeness of the polymers causes a mutual repulsion and greater opening of the layers (Al0h - 1.875 nm and Al14h 1.918 nm). The treatment with Al14h also resulted in pillars with more homogeneous heights (Table 1), as inferred from the

smaller width at half height (WHH) than in the other treatments (Selvaraj et al., 1996). Romero-Pérez et al. (2012) and Roca Jalil et al. (2014) employed the same procedure of Al14h and obtained similar results of $d(001)$ (ranging from 1.80 to 1.90 nm). In a different approach, Meunier (2007) and Velde and Meunier (2008) modeled diffractograms of pillared smectites with interstratification of 2:1 interlayers, randomly filled by polymers and also free of polymers. Due to the close spacing, they found that the reflexes tend to convolve, increasing the WHH and possibly changing the centroid and/or peak position. In this case, the decrease in WHH would also imply greater homogeneity in the distribution of the polymers among the mineral's interlayers.

The Al14h treatment resulted in more stable pillars (Table 1 and Figure 5). The $d(001)$ of this sample, after heated at 550 °C, was slightly higher than the Al0h treatment. The greater degree of occupancy of the interlayers by the pillars, the greater stability after heating because it depends on the degree of pillarization and not on the size homogeneity of the pillars (Selvaraj et al., 1996; Wen et al., 2019).

The complete interlayer filling by pillars (continuous sheet, mineral 2:1:1) increases the resistance to collapse when heated at 550 °C (Witthig and Allardice, 1986). Then, if there were no pillar formation in the PEG treatments, 14 h and 0 h, after heating at 550 °C the $d(001)$ should yield the same distance as natural MMT K^+ + 550 °C (1.24 nm) (Table 1). This would represent 0 % pillarization, allowing to estimate the percentage of contraction of each of the treatments. For example, heating of AlPEG decreased basal spacing from 1.794 to 1.596 nm. The complete collapse should be from 1.794 to 1.240 nm (natural MMT). The decrease, as a percentage of the maximum, was 36 % (index F, Table 1), which is equivalent to a pillarization of 64 % (index G, Table 1). The smaller pillarization of AlPEG was attributed to the competition between the Keggin ions and the PEG extending agent for the interlayer space. Treatment Al14h produced larger and more homogeneous size distribution of pillars in the interlayers. On the other hand, the greatest degree of filling of the interlayers by the pillars was obtained by the milder treatment Al0h (90 %) (Table 1). In the perspective of the interstratification model, these results indicate that the smaller degree of intercalation in Al14h allowed a greater number of free smectite layers, increasing the contribution of the larger spacings in the composition of the (001) peak and therefore, resulting in greater spacing of the convoluted peak .

The greater proportion of mineral particles in the silt fraction (68.7 %) explains the small SSA ($69 \text{ m}^2 \text{ g}^{-1}$) of the untreated MMT sample (Figure 8). Even smaller values of SSA ($20\text{-}64 \text{ m}^2 \text{ g}^{-1}$) for montmorillonite samples (sand and silt particles) were reported by other authors (Romero-Pérez et al., 2012; Gao et al., 2014; Roca Jalil et al., 2014; Bertella and Pergher, 2015). For a typical montmorillonite in the soil clay fraction, a SSA between 600 and 700 $\text{m}^2 \text{ g}^{-1}$ is expected (Jones, 1988).

The Al-hydroxy pillars increased the basal spacing and the surface area (SSA) became larger in the interlayer (Figure 8), since the lateral surface of the aluminum pillars (Keggin ion) also counted as internal surface area of the MMT. The inner area blocked by the top and bottom of the pillars in the tetrahedral sheet by Coulombic interactions (Čapková et al., 1998) is smaller than the increase in the internal area caused by the addition of the lateral surface of the Al-pillars. Other authors found similar SSA increase after pillarization by Al14h method in relation to the untreated MMT sample (Romero-Pérez et al., 2012; Roca Jalil et al., 2014). The lowest Al PEG SSA (Figure 8) was attributed to the filling of the interlayer space also by the PEG extending agent.

The CEC determined by the direct method of saturation of Mg^{2+} and exchange by Ba^{2+} was smaller ($85 \text{ cmol}_c \text{ kg}^{-1}$) (Figure 9) than those reported in the literature (approximately $100 \text{ cmol}_c \text{ kg}^{-1}$) (Borchardt, 1989; Wen et al., 2019), because the untreated MMT sample was an interlayered montmorillonite mineral with layers of chlorite or layers with a high degree of Al-hydroxy interlayered. The Li saturation caused an expressive decrease in CEC of the samples by neutralizing structural charges (the negative charge originated

from isomorphic substitution of Al^{3+} by Mg^{2+}). This electric field in the dioctahedral sheet makes the montmorillonite interlayer a thermodynamically unfavorable environment for uncharged, hydrophobic molecules (organic compounds) to escape from aqueous solutions (Johnston and Tombácz, 2002). However, due to the dioctahedral nature of montmorillonite, it was possible to neutralize those permanent negative charges (Greene-Kelly, 1953; Lim and Jackson, 1986) by inserting Li^+ into the empty octahedra (Figure 2). As a consequence, the dioctahedral sheet would have two Al^{3+} and one Li^+ for every three octahedral positions (Volzone, 1991), resulting in near-zero structural charge (Greene-Kelly, 1953).

CONCLUSIONS

The commercial sample purchased as bentonite was composed of montmorillonite interstratified with layers of chlorite or layers with a high degree of Al-hydroxy filling. This natural occupancy of the interstratified mineral caused an expressive reduction of CEC. The origin of the permanent CEC by isomorphic substitution did not occur only in the octahedral sheet, deviating from the theoretical model that differentiate montmorillonite from beidellite and nontronite by this property. Of the total permanent charges, 70 % occurred by replacing Al^{3+} by Mg^{2+} and 30 % by replacing Si^{4+} with Al^{3+} . Even with permanent charges on the tetrahedral sheet, the sample saturation with Li was efficient to neutralize the negative charges and render a non-expansive mineral.

The pillarization method using the PEG produced the smallest amount of stable pillars. The use of a milder pillarization method (AlOh), with smaller reagent concentration and contact time of the sample and solutions caused no prejudice to the formation of interlayered Al-hydroxy. In this method, the pillars produced have the greatest size uniformity. Thus, the AlOh method combined with the saturation with Li has been shown to be the best treatment (among those tested) to produce montmorillonite suitable to be used in the decontamination of polluted water with nonionic organic pollutants (such as pesticides and polycyclic aromatic hydrocarbons), since it caused the best stability of the interlayer spacing, increase of the specific surface area (SSA), and reduction of the cation exchange capacity (CEC).

AUTHOR CONTRIBUTIONS

Conceptualization:  Vander Freitas Melo (lead),  Regiane Salata (supporting), and  Gilberto Abate (supporting).

Methodology:  Vander Freitas Melo (lead),  Regiane Salata (supporting), and  Antonio Carlos Azevedo (supporting).

Software:  Vander Freitas Melo (supporting) and  Regiane Salata (lead).

Validation:  Vander Freitas Melo (lead),  Regiane Salata (supporting), and  Larissa Kummer (supporting).

Formal analysis:  Vander Freitas Melo (supporting),  Regiane Salata (lead),  Gilberto Abate (supporting),  Antonio Carlos Azevedo (supporting), and  Larissa Kummer (supporting).

Investigation:  Vander Freitas Melo (supporting) and  Regiane Salata (lead).

Resources:  Vander Freitas Melo (lead) and  Regiane Salata (supporting).

Data curation:  Vander Freitas Melo (supporting),  Regiane Salata (lead),  Gilberto Abate (supporting), and  Larissa Kummer (supporting).

Writing - original draft:  Vander Freitas Melo (lead),  Regiane Salata (supporting), and  Antonio Carlos Azevedo (supporting).

Writing - review and editing:  Vander Freitas Melo (lead),  Regiane Salata (supporting),  Gilberto Abate (supporting),  Antonio Carlos Azevedo (supporting), and Larissa Kummer (supporting).

Visualization:  Vander Freitas Melo (lead),  Regiane Salata (supporting),  Gilberto Abate (supporting),  Antonio Carlos Azevedo (supporting), and  Larissa Kummer (supporting).

Supervision:  Vander Freitas Melo (lead),  Regiane Salata (supporting),  Gilberto Abate (supporting),  Antonio Carlos Azevedo (supporting), and  Larissa Kummer (supporting).

Project administration:  Vander Freitas Melo (lead) and  Regiane Salata (supporting).

REFERENCES

- Azevedo AC, Vidal-Torrado P. Esmeclita, vermiculita, minerais com hidróxi entrecamadas e clorita. In: Melo VF, Alleoni LRF, editores. Química e Mineralogia do Solo - Parte I: Conceitos Básicos. Viçosa, MG: Sociedade Brasileira de Ciência do Solo; 2009. p. 381-426
- Barnhisel RI, Bertsch PM. Chlorites and hydroxy-interlayered vermiculite and smectite. In: Dixon JB, Weed SB, editors. Minerals in soil environments. Madison: Soil Science Society of America; 1989. p. 729-88.
- Batista AH, Melo VF, Gilkes R. Scanning and transmission analytical electron microscopy (STEM-EDX) identifies minor minerals and the location of minor elements in the clay fraction of soils. *Appl Clay Sci.* 2017;135:447-56. <https://doi.org/10.1016/j.clay.2016.10.032>
- Bertella F, Pergher SBC. Pillaring of bentonite clay with Al and Co. *Microp Mesop Mater.* 2015;201:116-23. <https://doi.org/10.1016/j.micromeso.2014.09.013>
- Bertsch PM. Conditions for Al₁₃ polymer formation in partially neutralized aluminum solutions. *Soil Sci Soc Am J.* 1987;51:825-8. <https://doi.org/10.2136/sssaj1987.03615995005100030046x>
- Borchardt G. Minerals in soil environment. In: Dixon JB, Weed SB, editors. Minerals in soil environments. Madison: Soil Science Society of America; 1989. p. 675-725.
- Bottero JY, Tchoubar D, Cases JM, Flessinger F. Investigation of the hydrolysis of aqueous solutions of aluminum chloride. 2. Nature and structure by small-angle X-ray scattering. *J Phys Chem.* 1982;86:3667-73. <https://doi.org/10.1021/j100215a034>
- Bujdák J. Effect of the layer charge of clay minerals on optical properties of organic dyes. A review. *Appl Clay Sci.* 2006;34:58-73. <https://doi.org/10.1016/j.clay.2006.02.011>
- Čapková P, Driessen RA, Numan M, Schenk H, Weiss Z, Klika Z. Modelling of intercalated clay minerals. *Chem Pap.* 1998;52:1-6.
- Chauhan M, Saini VK, Suthar S. Ti-pillared montmorillonite clay for adsorptive removal of amoxicillin, imipramine, diclofenac-sodium, and paracetamol from water. *J Hazard Mater.* 2020;399:122832. <https://doi.org/10.1016/j.jhazmat.2020.122832>
- Czímerová A, Bujdák J, Dohrmann R. Traditional and novel methods for estimating the layer charge of smectites. *Appl Clay Sci.* 2006;34:2-13. <https://doi.org/10.1016/j.clay.2006.02.008>
- Gao Y, Li W, Sun H, Zheng Z, Cui X, Wang H, Meng F. A facile in situ pillaring method-the synthesis of Al-pillared montmorillonite. *Appl Clay Sci.* 2014;88-89:228-32. <https://doi.org/10.1016/j.clay.2013.12.004>
- Gee GW, Bauder JW. Particle-size analysis. In: Kluter A, editor. Methods of soil analysis: Part 1 - Physical and mineralogical methods. 2nd ed. Madison: Soil Science Society of America; 1986. p. 383-411.

- Georgescu AM, Nardou F, Zichil V, Nistor ID. Adsorption of lead(II) ions from aqueous solutions onto Cr-pillared clays. *Appl Clay Sci.* 2018;152:44-50. <https://doi.org/10.1016/j.clay.2017.10.031>
- Greene-Kelly R. The identification of montmorillonoids in clays. *J Soil Sci.* 1953;4:233-7. [https://doi.org/10.1016/S0015-7368\(72\)70716-1](https://doi.org/10.1016/S0015-7368(72)70716-1)
- Hetzel F, Doner HE. Some colloidal properties of beidellite: Comparison with low and high charge montmorillonites. *Clays Clay Miner.* 1993;41:453-60. <https://doi.org/10.1346/CCMN.1993.0410406>
- Jaynes WF, Bigham JM. Charge reduction, octahedral charge, and lithium retention in heated, Li-saturated smectites. *Clays Clay Miner.* 1987;35:440-8. <https://doi.org/10.1346/CCMN.1987.0350604>
- Johnston C, Tombácz E. Surface chemistry of soil minerals. In: Dixon JB, Schulze DG, editors. *Soil mineralogy with environmental applications*. Madison: Soil Science Society of America; 2002. p. 37-67.
- Jones W. The structure and properties of pillared clays. *Catal Today.* 1988;2:357-67. [https://doi.org/10.1016/0920-5861\(88\)85015-6](https://doi.org/10.1016/0920-5861(88)85015-6)
- Karathanasis AD, Hajek BF. Evaluation of aluminum-smectite stability equilibria in naturally acid soils. *Soil Sci Soc Am J.* 1984;48:413-7. <https://doi.org/10.2136/sssaj1984.03615995004800020039x>
- Kaufhold S. Comparison of methods for the determination of the layer charge density (LCD) of montmorillonites. *Appl Clay Sci.* 2006;34:14-21. <https://doi.org/10.1016/j.clay.2006.02.006>
- Klug HP, Alexander LE. *X-Ray diffraction procedure: for polycrystalline and amorphous materials*. New York: John Wiley & Sons; 1954.
- Lahav N, Sham U, Shabtai J. Cross-linked smectites: I - Synthesis and properties of hydroxy-aluminum-montmorillonite. *Clays Clay Miner.* 1978;26:107-15. <https://doi.org/10.1346/CCMN.1978.0260205>
- Lim CH, Jackson ML. Expandable phyllosilicate reactions with lithium on heating. *Clays Clay Miner.* 1986;34:346-52. <https://doi.org/10.1346/CCMN.1986.0340316>
- Liu C, Cai W, Liu L. Hydrothermal carbonization synthesis of Al-pillared montmorillonite@ carbon composites as high performing toluene adsorbents. *Appl Clay Sci.* 2018;162:113-20. <https://doi.org/10.1016/j.clay.2018.06.005>
- Melo VF, Schaefer CEGR, Novais RF, Singh B, Fontes MPF. Potassium and magnesium in clay minerals of some Brazilian soils as indicated by a sequential extraction procedure. *Comm Soil Sci Plant Anal.* 2002;33:2203-25. <https://doi.org/10.1081/CSS-120005757>
- Meunier A. Soil hydroxy-interlayered minerals: a re-interpretation of their crystallochemical properties. *Clays Clay Miner.* 2007;55:380-8. <https://doi.org/10.1346/CCMN.2007.0550406>
- Mnasri-Ghnimi S, Frini-Srasra N. Removal of heavy metals from aqueous solutions by adsorption using single and mixed pillared clays. *Appl Clay Science.* 2019;179:105151. <https://doi.org/10.1016/j.clay.2019.105151>
- Moma J, Baloyi J, Ntho T. Synthesis and characterization of an efficient and stable Al/Fe pillared clay catalyst for the catalytic wet air oxidation of phenol. *RCS Adv.* 2018;8:30115-24. <https://doi.org/10.1039/C8RA05825C>
- Moore DM, Reynolds Jr RC. *X-Ray Diffraction and the identification and analysis of clay minerals*. New York: Oxford University Press; 1997.
- Roca Jalil ME, Baschini M, Rodríguez-Castellón E, Infantes-Molina A, Sapag K. Effect of the Al/clay ratio on the thiabendazol removal by aluminum pillared clays. *Appl Clay Sci.* 2014;87:245-53. <https://doi.org/10.1016/j.clay.2013.11.014>
- Romero-Pérez A, Infantes-Molina A, Jiménez-López A, Jalil ER, Sapag K, Rodríguez-Castellón E. Al-pillared montmorillonite as a support for catalysts based on ruthenium sulfide in HDS reactions. *Catal Today.* 2012;187:88-96. <https://doi.org/10.1016/j.cattod.2011.12.020>
- Sartor LR, Azevedo AC. Pillaring of clays and perspective of agronomic and environmental application and research. *Cienc Rural.* 2014;44:1541-8. <https://doi.org/10.1590/0103-8478cr20131536>

- Sartor LR, Azevedo AC, Andrade GRP. Study of colloidal properties of natural and Al-pillared smectite and removal of copper ions from an aqueous solution. *Environ Technol.* 2015;36:786-95. <https://doi.org/10.1080/09593330.2014.961564>
- Selvaraj S, Mohan BV, Krishna KN, Jai Prakash BS. Pillaring of smectites using an aluminium oligomer: A study of pillar density and thermal stability. *Appl Clay Sci.* 1996;10:439-50. [https://doi.org/10.1016/0169-1317\(95\)00039-9](https://doi.org/10.1016/0169-1317(95)00039-9)
- Sposito G. *The chemistry of soils.* New York: Oxford University Press; 1989.
- Sun L, Ling CY, Lavikainen LP, Hirvi JT, Kasa S, Pakkanen TA. Influence of layer charge and charge location on the swelling pressure of dioctahedral smectites. *Chem Phys.* 2016;473:40-5. <https://doi.org/10.1016/j.chemphys.2016.05.002>
- Tomlinson AAG. Characterization of pillared layered structures. *J Porous Mat.* 1998;5:259-74. <https://doi.org/10.1023/A:1009686322154>
- Vaughan DEW. Pillared clays - a historical perspective. *Catal Today.* 1988;2:187-98. [https://doi.org/10.1016/0920-5861\(88\)85002-8](https://doi.org/10.1016/0920-5861(88)85002-8)
- Velde B, Meunier A. *The origin of clay minerals in soils and weathered rocks.* New York: Springer; 2008.
- Volzone C. Improvements in the method to differentiate montmorillonite from other smectites. *J Mater Sci.* 1991;10:957-9.
- Wen K, Wei J, He H, Zhu J, Xi Y. Adsorption of lead(II) ions from aqueous solutions onto Cr-pillared clays. *Appl Clay Sci.* 2019;180:105203. <https://doi.org/10.1016/j.clay.2019.105203>
- Witthig LD, Allardice W. X-ray diffraction techniques. In: Kluter A, editor. *Methods of soil analysis: Part 1 - Physical and mineralogical methods.* 2nd ed. Madison: Soil Science Society of America; 1986. p. 331-62.